Bulletin of Mathematical Biology
https://doi.org/10.1007/s11538-019-00643-8

Society for Mathematical Biology

ORIGINAL ARTICLE

Conductance-Based Refractory Density Approach for a Population of Bursting Neurons

Anton Chizhov[1,2,3] · Fabien Campillo[3,4] · Mathieu Desroches[3,4] · Antoni Guillamon[3,5] · Serafim Rodrigues[3,6]

Received: 5 September 2018 / Accepted: 9 July 2019

Abstract

The conductance-based refractory density (CBRD) approach is a parsimonious mathematical–computational framework for modelling interacting populations of regular spiking neurons, which, however, has not been yet extended for a population of bursting neurons. The canonical CBRD method allows to describe the firing activity of a statistical ensemble of uncoupled Hodgkin–Huxley-like neurons (differentiated by noise) and has demonstrated its validity against experimental data. The present manuscript generalises the CBRD for a population of bursting neurons; however, in this pilot computational study, we consider the simplest setting in which each individual neuron is governed by a piecewise linear bursting dynamics. The resulting population model makes use of slow–fast analysis, which leads to a novel methodology that combines CBRD with the theory of multiple timescale dynamics. The main prospect is that it opens novel avenues for mathematical explorations, as well as, the derivation of more sophisticated population activity from Hodgkin–Huxley-like bursting neurons, which will allow to capture the activity of synchronised bursting activity in hyper-excitable brain states (e.g. onset of epilepsy).

Keywords Neuronal population · Conductance-based refractory density model · Intrinsically bursting neuron

✉ Serafim Rodrigues
srodrigues@bcamath.org

Anton Chizhov
anton.chizhov@mail.ioffe.ru

1 Ioffe Institute, Politekhnicheskaya str., 26, St. Petersburg, Russia 194021

2 Sechenov Institute of Evolutionary Physiology and Biochemistry of Russian Academy of Sciences, Torez pr., 44, St. Petersburg, Russia 194223

3 BCAM - Basque Center for Applied Mathematics, Bilbao, Bizkaia, Spain

4 Inria Sophia Antipolis Méditerranée, MathNeuro Team, Sophia Antipolis, France

5 Departament de Matemàtiques, Universitat Politècnica de Catalunya, Barcelona, Spain

6 Ikerbasque, Basque Foundation for Science, Bilbao, Spain

Published online: 16 July 2019

1 Introduction

An intense area of research in mathematical and computational neuroscience is the study of population dynamics of excitable neurons within a neuronal tissue as observed via electro-chemical observables. Advancing this topic constitutes a critical step which, if further progress is made, will provide insights as to how the brain orchestrates information and performs computations. Assuming the postulates put forth by the Hodgkin–Huxley formalism then it is arguably safe to say that single neuron activity is computationally understood. From a mathematical viewpoint, slow–fast theory has made considerable progress in characterising and classifying precisely the electrical patterns of single neurons. In contrast, the understanding of neuronal population dynamics lags behind and a number of approaches have been proposed to express macroscopic spatio-temporal observables (e.g. LFP, EEG, etc). To name a few, these approaches include Neural Mass models (Freeman 1972, 1975; Breakspear et al. 2005; Rodrigues et al. 2009; Marten et al. 2009), Firing rate models (Wilson and Cowan 1972; Chizhov et al. 2007), Neural Fields (Amari 1977; beim Graben and Rodrigues 2013; Avitabile et al. 2016), the Ott-Antonsen ansatz (Ott and Antonsen 2008; Montbrió et al. 2015), Population density models (Knight at al. 1996; Brunel and Hakim 1999; Knight et al. 2000; Nykamp and Tranchina 2000b; Apfaltrer et al. 2006; Ly and Tranchina 2007, 2009; Chizhov and Graham 2007, 2008) and Kinetic theory (Ventriglia 1974). The difficulty in progress is largely due to the fact that neurons are excitable open systems and there is strong coupling between the different temporal and spatial neuronal scales. The complex network synaptic connectivity shows lognormal distribution (with heavy tails) as well as extracellular characteristics. The temporal dynamics have a variety of oscillations (due to the neurons' intrinsic physiological properties).

In general, population density models for complex multidimensional neurons are expressed via multidimensional equations in partial derivatives (PDEs). In large-scale simulations, these multidimensional equations can lead to computational bottlenecks. Standard population density models do not attempt to reduce the dimensionality of these models. Presently, one of the stand-out paradigms for modelling neuronal populations is the refractory density (RD) approach, which belongs to the class of probability density methods (Knight et al. 2000). It is an efficient computational method to simulate neuronal populations (seen as statistical ensembles) of uncoupled neurons receiving similar input and dispersed by noise (or each neuron receiving individual Gaussian noise and a common for all neurons of a population, time-varying input). In first approximation, the RD method is akin to the methods developed in statistical physics, in particular the Boltzmann molecular chaos hypothesis, which allows to decorrelate elastic collisions between pairs of particles within a gas (due to conservation of momentum). As a consequence, it provides a plausible construct of a macroscopic description of the population by a single density. The RD method was first developed for simple, one-parametric integrate-and-fire-like neurons (Eggert and van Hemmen 2001; Gerstner and Kistler 2002). A significant step forward was taken by showing that the method could be extended for Hodgkin–Huxley-like neurons in Chizhov et al. (2006) and Chizhov and Graham (2007), which was then denoted as the conductance-based refractory density (CBRD) approach. The key point for consider-

ing Hodgkin–Huxley-like models is because these models have shown to provide good accurate approximations of neuronal firing and bursting as observed in a variety of experimental protocols that not only consider synaptic voltage-independent currents as an input but also synaptic conductances (Fernandez and White 2010; Smirnova et al. 2015), which is in contrast to the majority of simplified models that generally assume 1D input. These two inputs are crucial, which allow to relate to numerous experimental electrophysiological paradigms, experimental constraints (e.g. on neurophysiological parameters such as conductances) as those imposed in dynamic clamp, and therefore addressing questions imposed by these experimental setups. Having said that we note that progress is being made with new generation of simplified models with adaptive threshold dynamics, which have been shown to reproduce double-electrode current-clamp recordings (Gerstner and Naud 2009). While, these new generation models can be considered within the framework of the RD approach (Schwalger et al. 2017), we will still rely on the Hodgkin–Huxley neuron framework. Therefore, an important advantage of the CBRD approach is its computational efficiency, because it reduces the description of Hodgkin–Huxley neuron population to 1D transport equations, whereas the conventional probability density approach formally leads to computationally inefficient multidimensional PDEs.

The reduction to 1D PDEs in the CBRD approach (see Sect. 2.2) is possible due to a key insight, which is to parameterise the neuronal state variables by a single-phase variable, the time elapsed after spike t^* (Chizhov and Graham 2007). Specifically, the neuronal membrane voltages and possibly other neuronal state variables are functions of only time t and t^*. This is certainly valid for neurons with a renewal process at a spike (action potential), such as neurons modelled by integrate-and-fire models, spike-response (Gerstner and Kistler 2002) or fast-spiking neurons (Chizhov et al. 2006). It is approximately true for neurons with slow gating variables, like adaptive neurons (Chizhov and Graham 2007). This approximation is valid if the relaxation of each adaptive variable between spikes is roughly the same for different neurons within the population, which induces the inter-spike intervals of all neurons to become more or less comparable. Moreover, similarly to the typical RD approaches, an important assumption is to assume that all neurons within a population are governed by the same dynamics and are de-coupled, however are driven by the same input (possibly differentiated by noise). Thus, when a time-dependent input drives (in a similar fashion all neurons within the population), the state variables of the neurons, parameterised by t^*, fluctuate close to the average value of the population activity. This is the basis to split the problem into the solution of the equations for the average state variables and the fluctuations due to noise. The noise effect is captured by the so-called hazard function, which evaluates a probability for a single neuron to fire provided that the expected values of its states are known. The approximation of the hazard function was derived Chizhov and Graham (2007, 2008) by considering certain assumptions on the noise term. Interestingly, it is independent on the neuron model and substitutes former phenomenological approximations.

The CBRD has shown to be capable of modelling coupled/heterogeneous networks where each population node is a different CBRD model and more importantly has shown its validity in experimental studies. For example, a comparison of the CBRD model to a standard mean-field EEG model was made, which demonstrated improve-

ment gains (Chizhov et al. 2007) and subsequently, a number of modelling extensions followed. These included the case of temporally correlated noise (Chizhov and Graham 2008), two-compartment neurons (Chizhov 2014), lognormal distribution of input weights (Chizhov 2017) and finite-size population (Schwalger et al. 2017; Dumont et al. 2017). The validity of the CBRD method was also tested against data. In particular, it has modelled the visual cortex activity via two 2D layers of two-type populations that respond to both electrical and visual stimulation (Chizhov 2014). It has also provided insights in modelling epileptic discharges, such as, interictal discharges modelled via two populations (Chizhov et al. 2017), three populations with ionic dynamics for ictal discharges (Chizhov et al. 2019b), 2D lattice of two-type populations for spreading interictal discharges (Chizhov et al. 2019a).

In the present paper, we want to show that CBRD can be further extended to capture more complex electrical oscillations like bursting. Bursting neurons are characterised by the alternation between two distinct activity regimes, namely quiescent phases where the voltage slowly follows a quasi-steady-state and burst phases where groups of spikes are fired consecutively. There are two main modelling frameworks to capture bursting dynamics. The first framework corresponds to smooth continuous-time so-called *slow–fast* or *singularly perturbed* dynamical systems with at least three state variables, two fast and one slow. Indeed, in the context of *geometric singular perturbation theory (GSPT)* (Fenichel 1979; Jones 1995), the so-called *fast subsystem*, obtained as the slow variable is frozen and considered as a parameter, is a planar dynamical system with one distinguished parameter (the frozen slow variable). This planar system displays bistability between stable limit cycles and stable equilibria for a range of values of the frozen slow variable. What is more, this bistable region of the bifurcation diagram of the fast subsystem possesses a hysteretic loop, that is, a pair of bifurcations which connect in parameter space both families of attractors, equilibria and limit cycles. Hence, in the full system, the dynamics of the slow variable is organised (often through a feedback term involving one of the two fast variables) so that it oscillates in the region of bistability and switches between quasi-stationary (quiescent phase) to quasi-periodic (burst phase) regimes when slowly passing near the bifurcations of the fast subsystem that organises this hysteretic loop. Therefore, the two fast variables of a smooth bursting model account for the burst phase and the slow variable for the quiescent phase while also driving slowly (on average) the membrane potential through the burst; for more details, see Rinzel (1986) and Izhikevich (2000).

The second framework is that of *hybrid dynamical systems*, which are effectively a combination of smooth continuous-time dynamical systems together with a map. This map is applied to one or several variables each time they reach a predefined value (*threshold*), at which point the continuous-time system stops and these variables are mapped (instantaneously) to new values or *resets*. Classical example of hybrid neuron models is integrate-and-fire model (Knight 1972) where typically only the membrane potential gets reset upon threshold, which provides a spiking model with only one state variable (voltage). In the case of bursting neurons, hybrid models have two variables which both undergo reset upon threshold: membrane potential and a recovery variable which mimics gating dynamics. In this work, we consider for simplicity the *hybrid*

dynamical systems framework, but with an outlook for future work with the smooth case.

It is worth remarking that previous studies using the RD approach have also considered bursting neurons. However, we note that in these studies (for example, Casti et al. 2002), the derivation of the RD model from a simple bursting neuron retains the dimensionality of the neuronal equations. Moreover, an extension of this approach to more complex neurons would increase the dimension even more, which implies a loss in computational efficiency. In contrast, the CBRD approach always reduces the dimensionality, while fully representing the fast and slow variables of the underlying neuron model and therefore allows to model intrinsic bursting and is applicable to coupled populations and therefore offers significant advantages. To compare, in the setting of bursting dynamics with hybrid models, the RD approach gives rise to a 2D transport equation (as opposed to 1D transport for spiking regime). Moreover, the two state variables are parameterised by the time since last spike and the time since last burst. Specifically, the transport equations correspond to these two main state variables while the neuronal density describes neuronal dynamics and dispersion across population due to noise. The loss of computational efficiency in this case is probably the main reason as to why such 2D approach has not been developed (or attempted). However, we note that the dissipation is negligible during bursts because of their relatively short duration and high-conductance state that shunts the noisy currents. We make use of this property (as an advantage) to reduce the system to one-dimensional, and as a consequence, we obtain a computationally effective 1D RD model for a population of bursting neurons. The present work has to be seen as a pilot computational study, where for simplicity, we model bursting dynamics with hybrid models. However, we envisage that this work will stimulate the use of smooth slow–fast systems and will provide future challenging mathematical questions as well as the possibility of testing experimental data from bursting populations.

2 Methods

2.1 Single Neuron Model: Leaky Integrate-and-Fire Neuron with Noise

The framework setting under which we start our work is with hybrid dynamical systems but with the future outlook to develop and enhance it to smooth continuous-time *slow–fast* systems and their corresponding conductance (Hodgkin–Huxley) equivalent models. To this end, our starting point is the LIF spiking neuron model (i.e. hybrid dynamical system) since we will show that when we pass onto the bursting hybrid model, many of the LIF features will be retained within the macroscopic refractory density formulation. Specifically, the LIF neuron is given by the equation

$$C\,\frac{\mathrm{d}V}{\mathrm{d}t} = -(g_L + s(t))(V - V_{\mathrm{rest}}) + I(t) + \sigma_I\,\xi(t), \tag{1}$$

where $\xi(t)$ is a Gaussian white noise process characterised by its mean value, $\langle \xi(t) \rangle = 0$, and auto-correlation $\langle \xi(t)\xi(t') \rangle = C/g_L\ \delta(t - t')$; the standard deviation, σ_I, is

the noise amplitude. The neuron fires when the potential V crosses a threshold U_T. Immediately after a spike, V is reset to V_{reset}. The LIF neuron is characterised by the capacitance C and the leak conductance g_L. The input is determined by two signals, the synaptic current measured at the voltage level equal to V_{rest}, $I(t)$ and the total synaptic conductance $s(t)$. The effective membrane time constant is $\tau_m = C/(g_L + s(t))$.

We can then derive the equations of motion for a population of an infinite number of Eq. (1)-based LIF neurons receiving a common 2D input $[I(t), s(t)]$ and noise, individual for each neuron. The population firing rate is defined as a sum of all spikes, n^{act}, from neurons of the population over a short time window Δt, divided by the number of neurons N. After taking the limits of $N \to \infty$ and $\Delta t \to 0$, the firing rate ν is obtained as

$$\nu(t) = \lim_{\Delta t \to 0} \lim_{N \to \infty} \frac{1}{\Delta t} \frac{n^{\text{act}}(t;\ t + \Delta t)}{N}. \tag{2}$$

The direct approach to calculate the firing rate is via Monte Carlo simulations.

2.2 Population Model: CBRD Approach for Integrate-and-Fire Neurons

The firing rate for a population of LIF neurons receiving a common deterministic input and Gaussian noise is well approximated by the CBRD model Chizhov and Graham (2007) and Chizhov and Graham (2008). The CBRD model is expressed by a system of transport equations for two variables: the neuronal density in t^*-space $\rho(t, t^*)$, so-called refractory density, and $U(t, t^*)$, the membrane potential averaged across noise realisations, where t^* is the time elapsed since the last spike. The state of each neuron is parameterised by this phase variable. For the particular case of a LIF neuron, its only state variable is $V(t, t^*)$ (with its mathematical expectation $U(t, t^*)$). (For more complex neuron models, the gating variables of ionic channels are also parameterised by t^*, which allows to preserve the number of independent variables and thus leads to 1D PDEs (see Sect. 3.4).) This parameterisation leads to a reduced description with only one phase variable, which nevertheless preserves the information about neuronal states, provided all neurons they are subject to the same input history. The equation for $U(t, t^*)$ is derived from the original ordinary differential Eq. (1) by substituting the total derivative in time by a sum of partial derivatives: $\mathrm{d}/\mathrm{d}t = \partial/\partial t + \partial/\partial t^*$. The equation for $\rho(t, t^*)$ is derived from the neuron number conservation law $\partial\rho/\partial t + div\, \rho v = -\rho H$, where div is the divergence operator in the coordinate space (t^*-space); v is the velocity of neuronal flux in the t^*-space, which is $v \equiv \mathrm{d}t^*/\mathrm{d}t$ and equal to 1 by the definition of t^*, i.e. $v \equiv 1$. The expression $-\rho H$ is the source term that describes firing, where $H = H(U(t, t^*), s(t))$ is the probability for a single neuron to fire and $s(t)$ is a synaptic conductance which together with $I(t)$ drives equally all neurons within a population; for details, see our earlier work (Chizhov and Graham 2007) and further information that is provided below. Finally, the equations for $\rho(t, t^*)$ and $U(t, t^*)$ are as follows:

$$\frac{\partial \rho}{\partial t} + \frac{\partial \rho}{\partial t^*} = -\rho H(U(t, t^*), s(t)), \tag{3}$$

$$C\left(\frac{\partial U}{\partial t}+\frac{\partial U}{\partial t^*}\right)=-(g_L+s(t))(U-V_{\text{rest}})+I(t), \tag{4}$$

where I is the synaptic current; g_L is the leak conductance, C is the membrane capacitance and t^* is a time parametrisation, which denotes the time since last spike. The boundary conditions are

$$\nu(t)\equiv\rho(t,0)=\int_{+0}^{\infty}\rho H\,\mathrm{d}t^* \quad \text{and} \quad U(t,0)=V_{\text{reset}},$$

where $\nu(t)$ is the population firing rate. When calculating the dynamics of a neural population, the integration of Eq. (4) defines at each time moment t the distribution of deterministic (i.e. devoid from noise) voltage U along t^*. Then, the effect of threshold crossing and diffusion by noise are taken into account by the so-called hazard function (H-function), and the result of the integration of Eq. (3) is expressed in the distribution of ρ along t^* and the firing rate ν.

It is worth emphasising the rationale behind splitting the input signals into common inputs $(I(t), s(t))$, which all neurons are subject to and the effects of individual noise for each neuron and in turn how this leads to the H-function. We emphasise this because our approach is markedly in contrast to other probability density frameworks, for example, as described in Apfaltrer et al. 2006 that leads to a 2D probability density as opposed to ours which results in a 1D probability density. The central idea behind splitting is as follows. First, the common signals can be of any kinetic form. The individual noise can either be instantaneous (e.g. Gaussian white noise) or noise current (e.g. Ornstein-Uhlenbeck process), and in both cases, the noise effect is captured by the hazard function; for derivations, see Chizhov and Graham 2007, 2008. Secondly, only voltage fluctuations affect threshold crossing, thus only the fluctuations of membrane potential are considered. The voltage fluctuations around the mean voltage are governed by a linearised stochastic voltage equation, which is the same for different type neurons. The associated Langevin equation is equivalent to its alternative Fokker–Planck (FP) representation (1D for white noise and 2D for coloured noise) and is governed by the mean membrane potential $U(t)$ and mean membrane conductance $s(t)$. The hazard function is derived as a solution of the first-time passage problem based on the Fokker–Planck equation for the statistical distribution of voltage fluctuations due to white Gaussian noise near the deterministic mean potential U (Chizhov and Graham 2007). The problem has exact analytical solutions in two particular cases. In the first case of stationary stimulation, when U and s are constant, the solution is self-similar, with a constant shape distribution for a given value of U. Thus, the Fokker–Planck equation is reduced to an analytically solvable ordinary differential equation. In the second extreme case of an abrupt excitation with $\mathrm{d}U/\mathrm{d}t \to 0$, the solution is obtained from a frozen Gaussian distribution passing the threshold. As shown in Chizhov and Graham 2007, a solution for H in an arbitrary case is well approximated by a sum of the two extreme solutions. This solution is universal for different single neuron models; it was approximated with a relatively simple function of U varying in time t at a given t^*, depending as well on σ_I, U_T and $s(t)$:

$$
\begin{aligned}
H(U(t,t^*),s(t)) &= \frac{1}{\tau_m}\big(A(t,t^*)+B(t,t^*)\big),\\
A(t,t^*) &= \exp(6.1\cdot 10^{-3} - 1.12\,T - 0.257\,T^2 - 0.072\,T^3 - 0.0117\,T^4),\\
B(t,t^*) &= -\frac{2\,\tau_m}{\sqrt{\pi}}\left[\frac{\mathrm{d}T}{\mathrm{d}t}\right]_+ \frac{\exp(-T^2)}{1+\mathrm{erf}(T)},\\
T(t,t^*) &= \frac{U_T - U(t,t^*)}{\sqrt{2}\,\sigma_V}, \quad \sigma_V = \frac{\sigma_I}{\sqrt{2\,g_L(g_L+s(t))}}.
\end{aligned}
\tag{5}
$$

In our simulations, unless otherwise stated, we will consider $U_T = 0, s(t) \equiv 0, \tau_m = 1$ and $g_L = 1$.

3 Results

3.1 Single Neuron Model: Simple Bursting Neuron

For the bursting neuron dynamics, we consider a modified version of the model developed in Izhikevich (2003) and analysed in Coombes et al. et al. (2012) (using a piecewise linear approximation). The equations are defined as follows

$$\frac{\mathrm{d}V}{\mathrm{d}t} = |V| - a + I(t) - s(t)V, \tag{6}$$

$$\tau_a \frac{\mathrm{d}a}{\mathrm{d}t} = -a, \tag{7}$$

$$\text{if} \quad V > V_{\text{th}} \ \text{ then } \ V = V_{\text{reset}}, \ \ a = a + \Delta a, \tag{8}$$

with parameters set to the following values:

$$V_{\text{th}} = 1, \ V_{\text{reset}} = 0.2, \ \tau_a = 75, \ \Delta a = 4/75, \ I = 0.1.$$

These equations define a hybrid model with a planar piecewise linear (PWL) vector field together with a map, defined by reset conditions for the membrane voltage V, as well as an increment for a recovery variable a. The fact that $\tau_a \gg 1$ induces a timescale separation in the model, where the membrane potential V acts as a fast variable, while the recovery variable a is, in comparison, slower. The algebraic conditions (i.e. reset conditions) enable the emergence of limit cycle dynamics in the model, more specifically bursting oscillations (i.e. the dynamics converge to an attracting cycle instead of exploding in finite time). As depicted in Fig. 1 (bottom panel), the V-shaped PWL fast nullcline (so-called *critical manifold* S_0 of the system) has two branches, the left one is attracting and the right one is repelling. The dynamics along the left (attracting) branch of S_0 is slow and corresponds to the subthreshold part of the bursting cycle shown in Fig. 1 (bottom panel). Outside of the reset zone, the dynamics of the slow variable a is always decaying, which implies that once in the vicinity of the left branch of S_0, the trajectory moves slowly down towards the corner point of S_0, where its attractivity changes. Then, as typical in slow–fast systems near points where

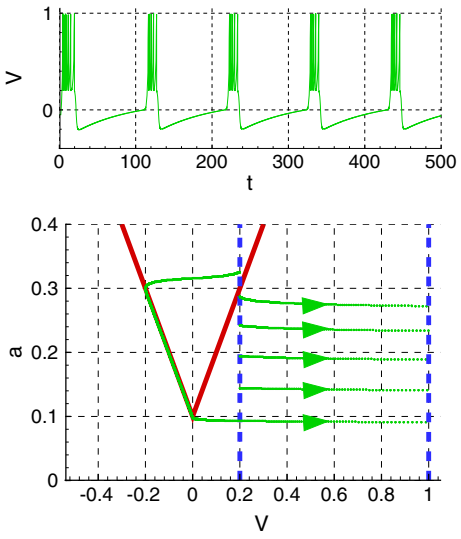

Fig. 1 (Color figure online) Hybrid model for bursting neuron. Voltage trace (top) and phase-space plot (bottom) with nullclines (red and blue) and a trajectory (green). The red nullclines intersect at hyperplane $V = 0$, which corresponds to the true neurophysiological threshold (seen from the perspective of smooth continuous-time slow–fast systems). The dashed blue line (left) corresponds to the V_{reset} and the dashed blue line (right) corresponds to V_{th}

a one-dimensional critical manifold changes from being attracting to being repelling (where so-called *normal hyperbolicity* fails), the overall dynamics switch from slow to fast and gets away from S_0 on the fast timescale.

This transition past, the two reset conditions allow for fast oscillations in between V_{reset} and V_{th} as long as the intersection point of the trajectory with the reset line $\{V = V_{\text{reset}}\}$ stays below the right branch of S_0, where the flow points rightwards towards the threshold line $\{V = V_{\text{th}}\}$. However, the reset also affects the slow variable a by incrementing its value each time by a quantity Δa. After a number of fast oscillations in between V_{reset} and V_{th}, the intersection point between the trajectory and the reset line crosses the right branch of S_0, where the flow now points leftwards. As a result, the trajectory goes back to the attracting branch of S_0 where slow dynamics, corresponding to the quiescent phase of the bursting cycle, resumes again.

Note that the notion of threshold for such IF models slightly differs from what is typically meant by threshold in their smooth counterparts, which then corresponds more to the *excitability threshold* of the membrane model. Indeed, models such as system (6) would explode in finite time without a reset in the membrane potential as it would grow unboundedly past the kink at $V = 0$. The threshold value V_{th} is introduced simply to avoid that the system explodes and to mark the occurrence of a spike (i.e. this is not a strict threshold in neurophysiological terms). The value V_{th} is higher than the V-level that one would want to associate with the excitability threshold. This is done so as to ensure that multiple spikes can be fired successively, hence mimicking a burst. In the context of smooth bursting models such as the extended Morris–Lecar system studied in Terman (1991), the reset value V_{reset} corresponds to the approximate minimum along the families of limit cycles of the fast subsystem. In such smooth bursters, with a similar geometry as system (6)–(8), the excitability threshold corresponds instead to a small perturbation of the unstable branch of the V-nullcline and is well captured by a so-called *maximal canard segment* (Desroches et al. 2013). More precisely, for

system (6)–(8), the excitability threshold can be approximated by a perturbation of order $1/\tau_a$ of the right branch of the V-nullcline.

A complete analysis of the bursting dynamics of system (6)–(8) is beyond the scope of the present work and will be an interesting topic for future work. In particular, it is convenient to focus on slow–fast spike-adding mechanisms present in this model, which allow to understand the burst size and timing. Already, as we will see below, the CBRD method can capture bursting dynamics within a population of neurons of the type given by system (6)–(8) with the noise as in (1). For a population, we set the noise amplitude to be $\sigma_I = 0.02\sqrt{2}$ (i.e. $\sigma_V = 0.02$).

3.2 CBRD Model for Simple Bursting Neurons

To derive the CBRD for bursting neurons, we additionally require an extra time parameter, say t^{**}, which denotes the time since last neuronal bursting activity. Relying on the Hybrid model (6)–(8) and its corresponding phase-plane diagram shown in Fig. 1, then t^{**} quantifies the time spent by the trajectory between the termination of the last spike (belonging to the previous burst) until the moment the trajectory reaches the hyperplane $V = 0$, corresponding to the apex where the two red nullclines intersect. The time parameter t^* has the same meaning as in previous work, where it denotes the time since last spike (i.e. defined as the time moment when V reaches V_{th}). However, we note that during bursting activity, t^* can be neglected because realistic neurons are driven towards high-conductance states and as a consequence noise is shunted. The fact that noise is shunted during burst implies that there is no need to evaluate the hazard function and describe the density leak during bursts. Moreover, the neurons become perfectly synchronised within a burst (i.e. the distribution along t^* is a delta function). Thus we drop t^*, but rename t^{**} as t^* for convenience. To discriminate the neuronal states where the noise is functioning and where it is not, we introduce a discrete state variable $\phi(t, t^*)$ that describes the states, either bursting or quiescent (leak), according to the (V, a)-plane (Fig. 1). The variable $\phi(t, t^*)$ takes discrete states of either 1—"leak", obtained when voltage $U(t, t^*)$ decreases below the boundary $U = 0$, or 0—"burst", obtained at the onset of a burst. Moreover, we assume that the slow variable a is reset at $t^* = 0$ to a some constant or variable $a_{\text{reset}}(t)$ to be given below.

Consequently, Eqs. (3)–(4) for the neuron based on Eq. (6)–(7) instead of Eq. (1) is obtained as follows:

$$\frac{\partial \rho}{\partial t} + \frac{\partial \rho}{\partial t^*} = -\rho H(U)\,\phi, \tag{9}$$

$$\frac{\partial U}{\partial t} + \frac{\partial U}{\partial t^*} = -|U| - a + I(t) - s(t)U + \delta(U - V_{\text{th}})(V_{\text{reset}} - V_{\text{th}}), \tag{10}$$

$$\frac{\partial a}{\partial t} + \frac{\partial a}{\partial t^*} = -\frac{a}{\tau_a} + \delta(U - V_{\text{th}})\,\Delta a, \tag{11}$$

$$\frac{\partial \phi}{\partial t} + \frac{\partial \phi}{\partial t^*} = -\delta(U)\,\phi, \tag{12}$$

The H-function is effective only for $\phi = 1$.

The firing rate is defined as a sum of all neurons that reached spike threshold:

$$\nu(t) = \int_{+0}^{\infty} \rho(t, t^*)\, \delta(U(t, t^*) - V_{\text{th}})\, \mathrm{d}t^* \tag{13}$$

The boundary conditions at the onset of burst are as follows:

$$\rho(t, 0) = \int_{+0}^{\infty} \rho H\, \mathrm{d}t^*, \tag{14}$$

$$U(t, 0) = V_{\text{reset}}, \tag{15}$$

$$a(t, 0) = a_{\text{reset}}, \tag{16}$$

$$\phi(t, 0) = 1 \tag{17}$$

The additional parameter is a_{reset}, which approximates a just before a burst if it initiates at the current time t. Indeed, a_{reset} tends to approach the value at the kink point of the red nullclines shown in Fig. 1. The kink point is given by the zero of the right-hand side of Eq. (6) for a single neuron, where $V = 0$, as well. From this, we would get $a_{\text{reset}} = I(t)$. However, this condition may lead to fast variation of a_{reset}, if $I(t)$ changes fast. Thus, we introduce an approximation $a_{\text{reset}} = (1 + s(t))\, U(t, t^* = \infty)$, which is valid because $U(t, t^* = \infty)$ is close to the term $I(t)/(1 + s(t))$ averaged over time period of 1 (i.e. normalised time period), which follows from the zeroed right-hand side of Eq. (10).

3.3 Single Neuron Model: Bursting Neuron with Potassium Current

As an example of a more complex bursting neuron model with conductance-based description of ionic currents, we add to the model Eqs. (6)–(8) a potassium current $I_K(V, t)$, adopted from Yu et al. (2008). For this, Eq. (6) is rewritten as

$$\frac{\mathrm{d}V}{\mathrm{d}t} = |V| - a + I_K(V, t) + I(t) - s(t)V, \tag{18}$$

where the potassium current is approximated as follows

$$I_K(V, t) = -g_K\, n(V, t)\, (V - V_K), \tag{19}$$

$$\frac{\mathrm{d}n}{\mathrm{d}t} = \frac{n_\infty - n}{\tau_n}, \tag{20}$$

$$n_\infty(V) = \frac{\alpha}{\alpha + \beta}, \quad \tau_n(V) = \frac{1}{\alpha + \beta}, \tag{21}$$

$$\alpha(V) = \frac{2(-V + 0.85)}{\exp\left((-V + 0.85)/0.09\right) - 1}, \tag{22}$$

$$\beta(V) = \frac{V - 0.85}{\exp\left((V - 0.85)/0.09\right) - 1}. \tag{23}$$

The integrate-and-fire model requires an additional reset condition:

$$\text{if } V > V_{\text{th}} \text{ then } n = 0.5. \tag{24}$$

The parameters are $g_K = 0.015$, $V_K = -0.3$ and $n_{\text{reset}} = 0.5$. After a spike, the voltage is partially reset due to the potassium channel; that is why V_{reset} is set to be larger, $V_{\text{reset}} = 0.5$.

3.4 CBRD Model for Bursting Neurons with Potassium Current

Generalisation of the CBRD model based on Eqs. (9)–(17) to more realistic neurons with explicit approximation of different ionic currents requires to account for the currents in Eq. (10) and adding the equations for the ionic channel gating variables. For a population of neurons with potassium channels, the equation for the refractory density Eq. (9) remains the same and Eq. (10) is substituted by

$$\begin{aligned}\frac{\partial U}{\partial t} + \frac{\partial U}{\partial t^*} = &-|U|-a - g_K n(V - V_K) + I(t)-s(t)U \\ &+ \delta(U - V_{\text{th}})(V_{\text{reset}} - V_{\text{th}}).\end{aligned} \tag{25}$$

Additionally, the following equation for the potassium gating variable n is derived from Eq. (20)

$$\frac{\partial n}{\partial t} + \frac{\partial n}{\partial t^*} = \frac{n_\infty - n}{\tau_n}, \tag{26}$$

with the supplementary expressions Eqs. (21), (22) and the boundary condition

$$n(t, 0) = n_{\text{reset}}. \tag{27}$$

The remaining equations are Eqs. (11)–(17), which completes the description. Note that the parameterisation of n by t^* helped to preserve the dimension of PDEs.

3.5 Simulations

Simulations with the CBRD model (Eqs. 3–5) for the LIF neuron population are shown in (Fig. 2). Here, we test the CBRD by considering two test problems, namely, stimulation with a current step and a complex input, which demonstrate that CBRD accurately reproduces the solutions obtained with the Monte Carlo simulations (Fig. 2). As an example of a complex-shaped input, we consider a sinus with an increasing frequency (Fig. 2d) as the current $I(t)$, and the absolute function of similar sinus function with twice smaller frequency as the conductance $s(t)$ (Fig. 2d). Note that the model performs well in the case of stimulation by both the voltage-independent current $I(t)$ and the conductance $s(t)$.

We subsequently simulate the CBRD model for simple bursting neurons (Eqs. 9–17) for a test problem of a current step stimulation (Fig. 3a). The firing rate as a population

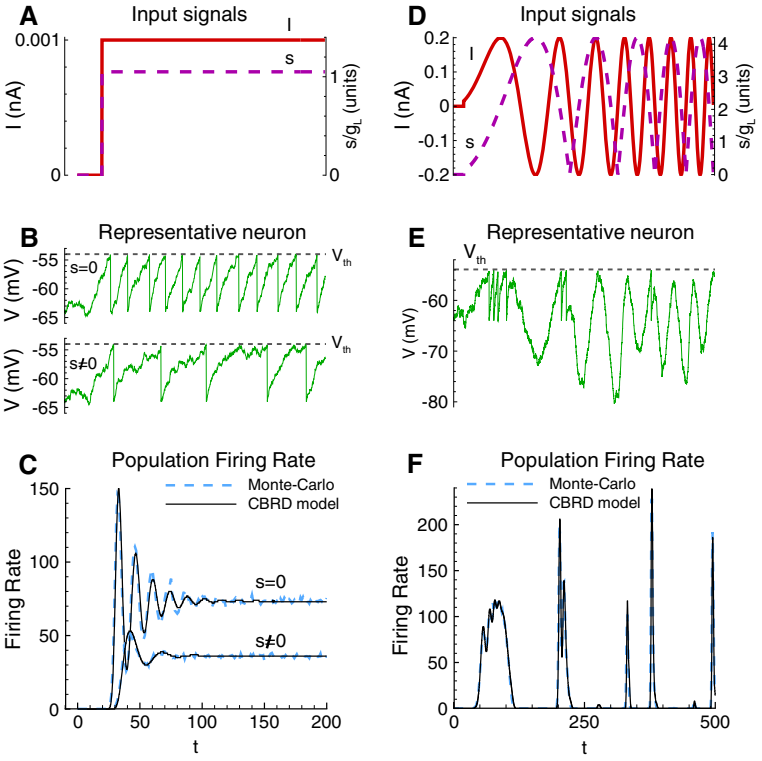

Fig. 2 (Color figure online) Population of LIF neurons. **a**–**c** Response to stepwise stimuli. **d**–**f** Response to a complex-shaped current. **a**, **d** Input current $I(t)$ and conductance $s(t)$. **b**, **e** Membrane voltage of a single neuron. **c**, **f** Population firing rate, calculated in Monte Carlo simulation and the CBRD model. 50000 trials were used in the Monte Carlo simulations

response to the stimulus is shown in Fig. 3c. The corresponding voltage response of an individual neuron is depicted in Fig. 3b. Due to synchronised initial state of the neurons within the population, the first burst turns out to be hyper-synchronous. Peaks of the firing rate during the first burst correspond to separate spikes. At the interval between the first and second burst, neuronal states desynchronise, which gives rise to a smoothing effect of the firing rate in subsequent bursts. In fact, this smoothing effect amplifies in subsequent bursts and thus a total desynchronisation occurs. The firing rate obtained with the population model is compared to the one from Monte Carlo simulation (Fig. 3c), which shows satisfactory agreement, though showing weaker fading of the response oscillations. An important property of the proposed model is that the timing of the population firing rate bumps is reproduced accurately.

We note that the voltage U does not depend on ν. As a consequence, for constant step stimulation, the voltage profile in t^*-space is stationary (Fig. 4b). The corresponding time profile in t^*-space is shown (as green) in Fig. 4c. At t^* close to 100 ms, the voltage approaches the threshold (orange). As a consequence, and according to Eq. (5), the hazard function increases (blue). As expected, this implies that a significant fraction of neurons with t^* close to 100 ms switch to the bursting phase, upon which there

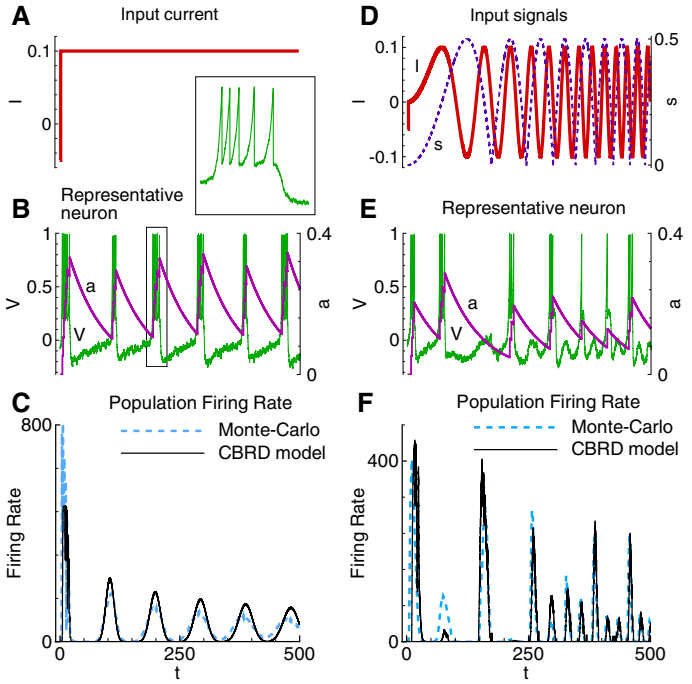

Fig. 3 (Color figure online) Population of bursting neurons. **a**–**c** Response to a step of current. **d**–**f** Response to a complex-shaped current. **a**, **d** Input current $I(t)$ and conductance $s(t)$. **b**, **e** Membrane voltage of a single neuron. The green traces are the voltage responses, while the time trajectory of the recovery variable, a is shown in purple. **c**, **f** Population firing rate, calculated in Monte Carlo simulation and the CBRD model. Twenty thousand trials were used in the Monte Carlo simulations

is a reset of t^* (i.e. $t^* = 0$). Moreover, according to Eq. (9), the neuronal density (red) decreases with t^* at t^* close to 100 ms and increases at $t^* = 0$. At t^* from 0 until about 80 ms, the neuronal density shifts to the right and then decays. Note that because the flux to the reset point $t^* = 0$ affects ρ and depends on it, the neuronal density converges to the steady state much slower than the voltage, as seen from the comparison between Fig. 4a, b.

The proposed model works with an arbitrary input. Again, we consider a complex-shaped input with variable current $I(t)$ and conductance $s(t)$ (Fig. 3d), as in Fig. 2d. A single neuron fires irregularly in response to such input (Fig. 3e). The firing rate obtained with the population model is well compared to the one from Monte Carlo simulation (Fig. 3f) in respect to qualitative behaviour with fading oscillations, the amplitudes of the firing rate peaks and the timing of the peaks. The residual difference is due to the approximate nature of two assumptions: the one about a_{reset} and the other one that neglects by the effects of noise during the bursts. Note that the second assumption would be more relevant to more realistic neurons with shunting, for which the noise effect vanishes at the high-conductance state during bursts.

Finally, we demonstrate that the CBRD model for bursting neurons with potassium current have similar qualitative behaviour (Fig. 5). The effect of the potassium current

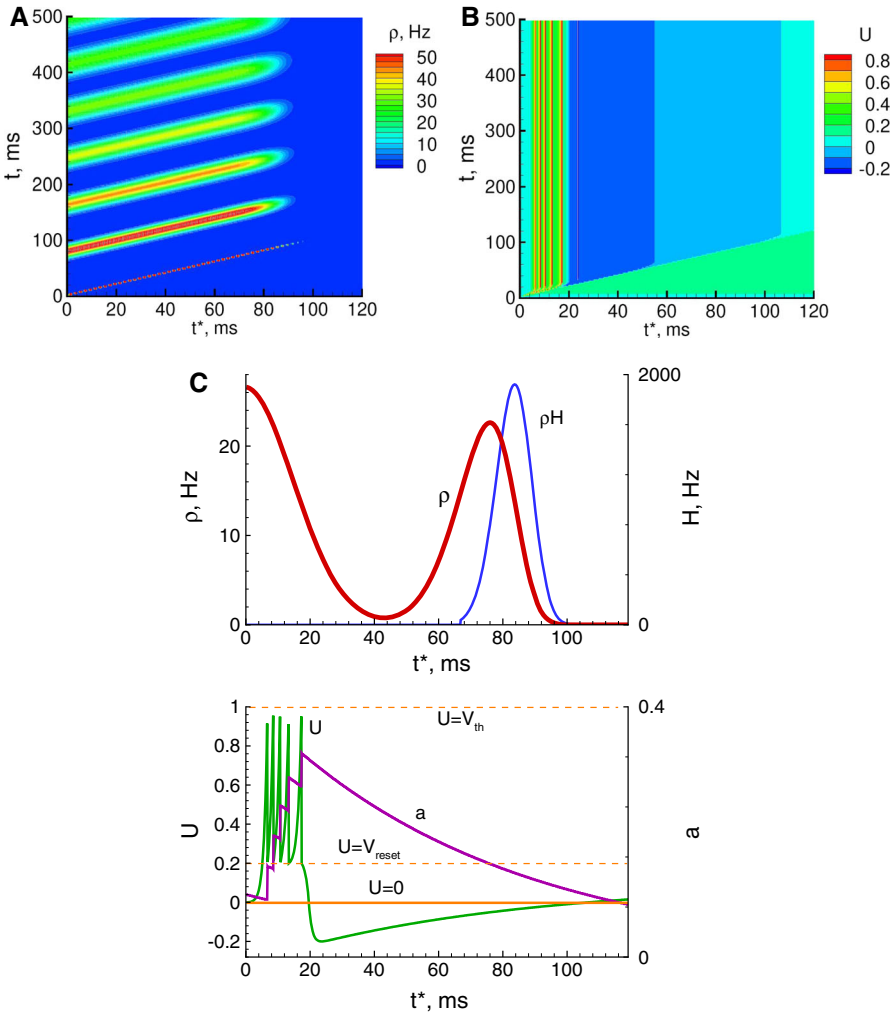

Fig. 4 (Color figure online) This plot extends Fig. 3a–c. Specifically, it depicts $t^* - t$-plots for the neuronal density ρ (**a**) and voltage U (**b**), that lead to the firing rate response shown in Fig. 3c. **c** Shows the profiles in t^*-space at $t = 500$ ms for the neuronal density ρ and the source term ρH (middle panel) and the mean voltage U and adaptation a (bottom panel)

on voltage is seen from comparison of the traces from the insets in Figs. 3b and 5b. After spikes, the voltage is partially reset due to the potassium channel. The potassium current is reset at each spike and it vanishes between the spike bursts. Qualitatively, the bursts are similar to those in the simple bursting model. The firing rate is similar to that for the simple bursting neuron population.

All together, these derivations and simulations demonstrate that CBRD framework can be extended to a population of intrinsically bursting neurons.

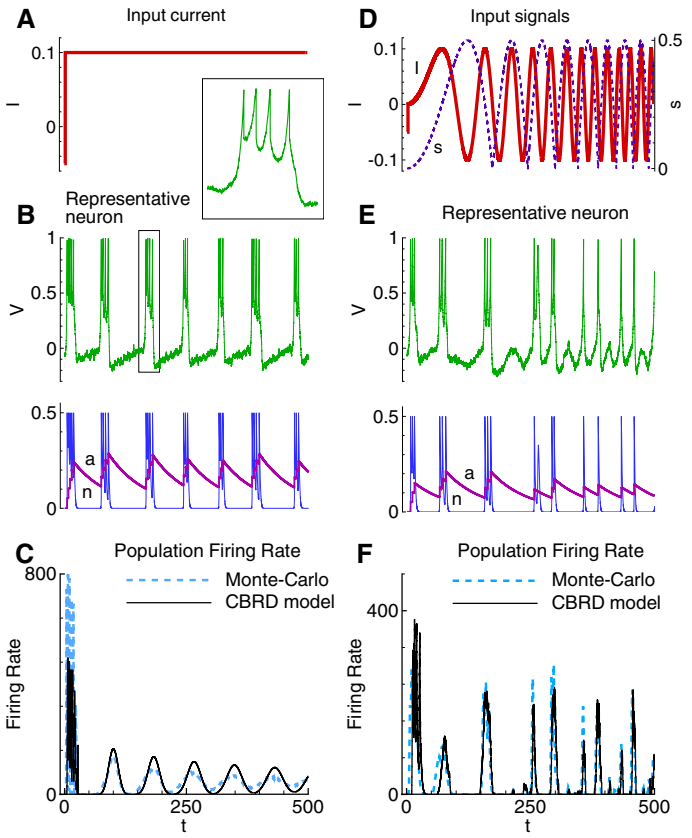

Fig. 5 (Color figure online) Population of bursting neurons with potassium current. **a**–**c** Response to a step of current. **d**–**f** Response to a complex-shaped current. **a**, **d** Input current $I(t)$ and conductance $s(t)$. **b**, **e** Membrane voltage of a single neuron. The green traces are the voltage responses, while the time trajectory of the recovery variable, a and the potassium gating variable n are shown in purple and blue, correspondingly. **c**, **f** Population firing rate, calculated in Monte Carlo simulation and the CBRD model. Twenty thousand trials were used in the Monte Carlo simulations

3.6 Discussion

This is a preliminary computational study that demonstrates the plausibility of extending CBRD framework towards bursting dynamics. There are however a number of mathematical challenges (and further computational ones), as well as experimental validations to consider in the near future. From the mathematical viewpoint, it will be essential to analyse the properties of the nonlinear renewal system of Eqs. (9)–(11), in particular its asymptotic time behaviour (Perthame and Tumuluri 2008; Cañizo and Yoldaş 2018). Additionally, it will be interesting to bridge the CBRD (i.e. PDEs) proposed in the present paper with detailed piecewise deterministic Markov processes (PDMP) approaches where spike trains events are explicitly described with the help of stochastic point processes (Chevallier et al. 2015). Indeed, system (9)–(11) is the large population mean-field approximation of systems of coupled PDMP models. This will

help to assess the stochastic disparity between the two approaches in terms of martingale problems. In this perspective, an intermediate model could be proposed, as a stochastic PDE, using a diffusion approximation (Dumont et al. 2017).

Another future direction for the present work will be to enhance the slow–fast analysis of the single neuron model used in the population density model that we have proposed here. Indeed, CBRD for bursting models allows to finely analyse both the quiescent and the burst phases. In particular, their duration and timing can be more precisely estimated by combining the knowledge of the fast subsystem's bifurcation structure together with the slow oscillation that passes through it in the full system. Besides, this analysis can be simplified when the underlying model is piecewise linear (Desroches et al. 2016). Such a slow–fast study will shed further light onto the role of the two main parameters of the density model, namely time since last spike and time since last burst. Finally, the interactions between slow–fast timescales and stochasticity can be analysed using a mix of CBRD and probability theory (Berglund and Gentz 2006); we plan to extend the theoretical aspects of the modelling framework proposed in the present work by using such methods.

From a biophysics point of view, it will be worth to reinterpret the macroscopic neuronal density. In particular, note that the starting point of the CBRD is the assumption of a statistical ensemble of uncoupled neurons (possibly differentiated by noise). This assumption of uncoupled neurons invokes the Boltzmann molecular chaos hypothesis (also called Stosszahlansatz), where the collision of particles (effectively the coupling) is neglected. This is justified by the fact that the collisions are elastic and, due to conservation laws, the colliding gas particles effectively forget the effects of the previous collisions (i.e. collisions de-correlate exponentially fast). In this view, there is the tantalising question as to what would be the corresponding conservation law (if any) and in what physiological conditions would it be valid.

The proposed model has been validated by comparison with an alternative model, the Monte Carlo simulations. From an experimental point of view, it will be also important to validate the CBRD for bursting dynamics. We recall that the CBRD for spiking dynamics has been validated against data. Specifically, in a previous work carried out in Chizhov (2017), a CBRD model for adaptive, regular spiking neurons was compared with electrophysiological recordings in a single pyramidal cell, obtained by Tchumatchenko et al. (2011). These experiments were in whole-cell patch-clamp recordings, and the perturbation protocol followed a time-varying weak piecewise current (i.e. changing stepwise current) that was injected into the neuron. The statistics of spiking response were characterised by the post-stimulus spike-time histogram, which in the CBRD framework corresponds to the firing rate for a neuronal population. In simulations, the spike trains in response to stepwise current injection revealed that the CBRD model responses replicate and explain experimental neuronal responses, including the effects of the adaptation. Taking these experiments as a starting point, we propose similar future experiments for bursting cells, which we believe is feasible but has not yet been done. These envisaged experiments could then be compared to the bursting CBRD approach.

The probability density approach (PDA), and particularly the refractory density approach are an important class of modelling framework that have potential to solve neurobiological questions. For instance, a PDA-based model of a single population

revealed the effects of synaptic noise filtering by LIF neurons (Brunel et al. 2001). A problem of gain modulation in refractory integrate-and-fire neurons receiving an input with shunt-dependent fluctuations has been solved with the help of a PDA-based model (Ly and Doiron 2009). Networks of coupled excitatory and inhibitory integrate-and-fire neurons have been simulated with a PDA (Nykamp and Tranchina 2000a; Apfaltrer et al. 2006). The CBRD approach refines the PDA approach and has further shown to be well suited to efficiently study cortical activity and also to have good agreements with some experiments. For example, the CBRD has been applied to study the visual cortex activity (Chizhov 2014), where a cortical domain was considered as a layered continuum of interacting excitatory and inhibitory neuronal populations. The simulations allowed to reproduce evoked responses of the cortical network that were registered by the patch-clamp electrophysiological methods and the optical recordings performed in vivo. Another study with a CBRD model has revealed mechanisms of epileptic interictal discharges (Chizhov et al. 2017). In this study, the quality of the CBRD method was important to reproduce abrupt onset of spontaneous pulses of hyper-synchronised activity as observed by electrophysiological measurements. Aspects of spatial propagation of the interictal discharges have been further simulated in Chizhov et al. (2019a) and found to be consistent with paired patch-clamp recordings.

The CBRD approach proposed for simplified bursting neurons challenges a future derivation of more sophisticated population activity models for Hodgkin–Huxley-like bursting neurons, which will enable modelling of synchronised bursting activity in hyper-excitable brain states as epilepsy. It is well-known that an increase in intrinsic excitability can cause bursting in cells which usually fire single action potentials. Extracellular potassium concentration has been shown to modulate intrinsic excitability (Jensen and Yaari 1997). It is well established that the extracellular potassium concentration increases during epileptogenesis and may be critically involved in synchronised burst oscillations during seizures. Moreover, nonsynaptic, spontaneous activity switches from single spikes to bursting when the concentration is increased (Frohlich and Bazhenov 2006). With the proposed model, an application of the CBRD approach to study epilepsy may be extended to the case of significant contribution of intrinsically bursting cells.

Acknowledgements This research is supported by the Basque Government through the BERC 2018-2021 programme and by the Spanish State Research Agency through BCAM Severo Ochoa excellence accreditation SEV-2017-0718 and through Project RTI2018-093860-B-C21 funded by (AEI/FEDER, UE) and acronym "MathNEURO". SR would further like to acknowledge the support of Ikerbasque (The Basque Foundation for Science). Moreover, the research of AC was supported by the Russian Science Foundation Grant (Project 16-15-10201). The research of AG was supported by the Spanish Grant MINECO-FEDER-UE MTM-2015-71509-C2-2-R and the Catalan Grant Number 2017SGR1049. Finally, SR, FC and MD would like to acknowledge the support of Inria through the associated team project NeuroTransSF.

References

Amari SI (1977) Dynamics of pattern formation in lateral-inhibition type neural fields. Biol Cybern 27(2):77–87

Apfaltrer F, Ly C, Tranchina D (2006) Population density methods for stochastic neurons with realistic synaptic kinetics: firing rate dynamics and fast computational methods. Network 17(4):373–418
Avitabile D, Desroches M, Knobloch E (2016) Spatiotemporal canards in neural field equations. Phys Rev E 95(4):042205
beim Graben P, Rodrigues S (2013) A biophysical observation model for field potentials of networks of leaky integrate-and-fire neurons. Front Comput Neurosci 6:100
Berglund N, Gentz B (2006) Noise-induced phenomena in slow-fast dynamical systems: a sample-paths approach. Springer, Berlin
Breakspear M, Roberts JA, Terry JR, Rodrigues S, Mahant N, Robinson PA (2015) A unifying explanation of primary generalized seizures through nonlinear brain modeling and bifurcation analysis. Cerebral Cortex 16(9):1296–1313
Brunel N, Hakim H (1999) Fast global oscillations in networks of integrate-and-fire neurons with low firing rates. Neural Comput 11(7):1621–1671
Brunel N, Chance FS, Fourcaud N, Abbott LF (2001) Effects of synaptic noise and filtering on the frequency response of spiking neurons. Phys Rev Lett 86(10):2186–2189
Cañizo JA, Yoldaş H (2018) Asymptotic behaviour of neuron population models structured by elapsed-time. arXiv:1803.07062
Casti ARR, Omurtag A, Sornborger A, Kaplan E, Knight B, Victor J, Sirovich L (2002) A population study of integrate-and-fire-or-burst neurons. Neural Comput 14:957–986
Chevallier J, Cáceres MJ, Doumic M, Reynaud-Bouret P (2015) Microscopic approach of a time elapsed neural model. Math Models Methods Appl Sci 25(14):2669–2719
Chizhov AV (2014) Conductance-based refractory density model of primary visual cortex. J Comput Neurosci 36(2):297–319
Chizhov AV (2017) Conductance-based refractory density approach: comparison with experimental data and generalization to lognormal distribution of input current. Biol Cybern 111(5–6):353–364
Chizhov AV, Graham LJ (2007) Population model of hippocampal pyramidal neurons, linking a refractory density approach to conductance-based neurons. Phys Rev E 75:011924
Chizhov AV, Graham LJ (2008) Efficient evaluation of neuron populations receiving colored-noise current based on a refractory density method. Phys Rev E 77:011910
Chizhov AV, Graham LJ, Turbin AA (2006) Simulation of neural population dynamics with a refractory density approach and a conductance-based threshold neuron model. Neurocomputing 70:252–262
Chizhov AV, Rodrigues S, Terry JR (2007) A comparative analysis of a detailed neural population model and a mean-field EEG model. Phys Lett A 369:31–36
Chizhov AV, Amakhin DV, Zaitsev AV (2017) Computational model of interictal discharges triggered by interneurons. PLoS ONE 12(10):e0185752
Chizhov AV, Amakhin DV, Zaitsev AV (2019a) Spatial propagation of interictal discharges along the cortex. Biochem Biophys Res Commun 508:1245–1251
Chizhov AV, Amakhin DV, Zaitsev AV (2019b) Mathematical model of Na–K–Cl homeostasis in ictal and interictal discharges. PLoS ONE 14(3):e0213904
Coombes S, Thül R, Wedgwood KCA (2012) Nonsmooth dynamics in spiking neuron models. Physics D 241:2042–2057
Desroches M, Kaper TJ, Krupa M (2013) Mixed-mode bursting oscillations: dynamics created by a slow passage through spike-adding canard explosion in a square-wave burster. Chaos 23(4):046106
Desroches M, Guillamon A, Ponce E, Prohens E, Rodrigues S, Teruel AE (2016) Canards, folded nodes, and mixed-mode oscillations in piecewise-linear slow-fast systems. SIAM Rev 58(4):653–691
Dumont G, Payeur A, Longtin A (2017) A stochastic-field description of finite-size spiking neural networks. PLoS Comput Biol 13(8):e1005691
Eggert J, van Hemmen JL (2001) Modeling neuronal assemblies: theory and implementation. Neural Comput 13:1923–1974
Fenichel N (1979) Geometric singular perturbation theory for ordinary differential equations. J Differ Equ 31(1):53–98
Fernandez FR, White JA (2010) Gain control in CA1 pyramidal cells using changes in somatic conductance. J Neurosci 30(1):230–241
Freeman W (1972) Waves, pulses, and the theory of neural masses. Prog Theor Biol 2(1):1–10
Freeman W (1975) Mass action in the nervous system. Academic Press, Cambridge
Fröhlich F, Bazhenov M (2006) Coexistence of tonic firing and bursting in cortical neurons. Phys Rev E 74:031922

Gerstner W, Kistler WM (2002) Spiking neuron models: single neurons, populations, plasticity. Cambridge University Press
Gerstner W, Naud R (2009) How good are neuron models? Science 326:379–326
Izhikevich EM (2000) Neuronal excitability, spiking and bursting. Int J Bifurc Chaos 10(6):1171–1266
Izhikevich EM (2003) Simple model of spiking neurons. IEEE Trans Neural Netw 14(6):1569–1572
Jensen MS, Yaari Y (1997) Role of intrinsic burst firing, potassium accumulation, and electrical coupling in the elevated potassium model of hippocampal epilepsy. J Neurophysiol 77(3):1224–1233
Jones CKRT (1995) Geometric singular perturbation theory. In: Arnold L, Jones CKRT, Mischaikow K, Raugel G (eds) Dynamical systems, lecture notes in mathematics, vol 1609. Springer, Berlin, pp 44–118
Knight B (1972) Dynamics of encoding in a population of neurons. J Gener Physiol 59:734–766
Knight BW, Manin D, Sirovich L (1996) Dynamical models of interacting neuron populations. In: Gerf EC (ed) Symposium on robotics and cybernetics: computational engineering in systems applications. Cite Scientifique, Lille
Knight BW, Omurtag A, Sirovich L (2000) The approach of a neuron population firing rate to a new equilibrium: an exact theoretical result. Neural Comput 12:1045–1055
Ly C, Doiron B (2009) Divisive gain modulation with dynamic stimuli in integrate-and-fire neurons. PLoS Comput Biol 5(4):e1000365
Ly C, Tranchina D (2007) Critical analysis of dimension reduction by a moment closure method in a population density approach to neural network modeling. Neural comput 19(8):2032–2092
Ly C, Tranchina D (2009) Spike train statistics and dynamics with synaptic input from any renewal process: a population density approach. Neural Comput 21:360–396
Marten F, Rodrigues S, Benjamin O, Richardson MP, Terry JR (2009) Onset of polyspike complexes in a mean-field model of human electroencephalography and its application to absence epilepsy. Philos Trans R Soc A 367(1891):1145–1161
Montbrió E, Pazó D, Roxin A (2015) Macroscopic description for networks of spiking neurons. Phys Rev X 5:021028
Nykamp DQ, Tranchina D (2000a) A population density approach that facilitates large-scale modeling of neural networks: analysis and an application to orientation tuning. J Comput Neurosci 8:19–50
Nykamp D, Tranchina D (2000b) A population density approach that facilitates large-scale modeling of neural networks: analysis and application to orientation tuning. J Comput Neurosci 8:19–50
Ott E, Antonsen TM (2008) Low dimensional behavior of large systems of globally coupled oscillators. Chaos 18(3):037113
Perthame B, Tumuluri SK (2008) Selected topics in cancer modeling. In: Bellomo N, de Angelis E (eds) Nonlinear renewal equations. Springer, Berlin
Rinzel J (1987) A formal classification of bursting mechanisms in excitable systems. In: International congress of mathematicians, Berkeley, California, USA, August 3-11, 1986, volume II, pp 1578–1593. American Mathematical Society
Rodrigues S, Barton D, Szalai R, Benjamin O, Richardson MP, Terry JR (2009) Transitions to spike-wave oscillations and epileptic dynamics in a human cortico-thalamic mean-field model. J Comput Neurosci 27(3):507–526
Schwalger T, Deger M, Gerstner W (2017) Towards a theory of cortical columns: from spiking neurons to interacting neural populations of finite size. PLoS Comput Biol 13(4):e1005507
Smirnova EY, Zaitsev AV, Kim KKh, Chizhov AV (2015) The domain of neuronal firing on a plane of input current and conductance. J Comput Neurosci 39(2):217–33
Tchumatchenko T, Malyshev A, Wolf F, Volgushev M (2011) Ultrafast population encoding by cortical neurons. J Neurosci 31(34):12171–12179
Terman D (1991) Chaotic spikes arising from a model of bursting in excitable membranes. SIAM J Appl Math 51(5):1418–1450
Ventriglia F (1974) Kinetic approach to neural systems: I. Bull Math Biol 36(5–6):535–544
Wilson HR, Cowan JD (1972) Excitatory and inhibitory interactions in localized populations of model neurons. Biophys J 12(1):1–24
Yu Y, Shu Y, McCormick DA (2008) Cortical action potential back propagation explains spike threshold variability and rapid-onset kinetics. J Neurosci 28(29):7260–7272